ORIGINAL PAPER

Recycling of abrasives in abrasive water jet cutting with different types of granite

Gokhan Aydin

Abstract The cost of abrasives has restricted usage of abrasive water jet (AWJ) technology in natural stone cutting applications. However, recycling of the abrasives makes the technology more economical, effective, and environmentally friendly. In this study, significant rock properties affecting the recycling of abrasives in AWJ cutting of granites are investigated. Abrasive mass percentage above 106 μm ($AMP_{106\mu m}$) is considered as a performance criterion in terms of recycling of abrasives since these abrasives can be effectively reused in the rock cutting applications. The study reveals that a considerable amount of used abrasives is in a reusable form. Among the rock properties, the microhardness is statistically determined as the most significant rock property affecting the $AMP_{106\mu m}$. It is also concluded that the $AMP_{106\mu m}$ can be explained with high accuracy by the proposed model including the microhardness, the quartz content, and the plagioclase content.

Keywords Abrasive water jet · Rock · Abrasive · Recycling

Introduction

The use of natural stones has dramatically increased in the last few years worldwide. The growing commercial market and competition for natural stones have resulted in an increased demand for innovative manufacturing processes (Sengun and Altindag 2013; Ataei et al. 2012). Due to the composition of natural stones (especially granite), machining and processing with traditional systems have some difficulties (Mikaeil et al. 2013; Bayram 2012). Therefore, new cutting methods to increase machining efficiency by minimizing production time

G. Aydin (✉)
Department of Mining Engineering, Karadeniz Technical University,
61080 Trabzon, Turkey
e-mail: gaydin@ktu.edu.tr

and costs are required. Among the innovative manufacturing processes, abrasive waterjet (AWJ) cutting has developed a broad application area as an alternative technology to tradiitional systems in processing and machining of natural stones and most engineered materials (Aydin et al. 2011).

Many studies have been conducted on the AWJ technology and the cutting of natural rock and artificial rocklike materials with particular applications. The effects of some process parameters on the penetration of sandstones machined by high-speed AWJ were investigated by Brook and Summers (1969). A fine continuous high-pressure AWJ for coal and rock penetration was studied by Nikonov and Goldin (1972). Chakravarthy and Babu (1999) presented a fuzzy-based model and suggested a set of process parameters in the cutting of black granite by AWJ. Chakravarthy and Babu (1998) proposed an approach based on the principles of fuzzy logic and genetic algorithm for the selection of optimal process parameters in AWJ cutting of granite. Xiaohong et al. (2000) conducted experimental studies on rock cutting by collimated AWJ. An experimental study was carried out to determine the effect of material properties on the cutting mechanisms involved in AWJ of calcareous stones (Miranda and Quintino 2005). A relationship between declination angle and cutting wall quality was explained through experimentations (Hlavac et al. 2009). Ciccu and Grosso (2010) experimentally investigated the improvement of mechanical excavation performance by AWJ assistance (Ciccu and Grosso 2010). Effects of process parameters on the cut depth of granite were investigated, and statistical models were developed for the prediction of cut depth from process parameters (Pon Selvan and Raju 2011). Surface roughness of granite cut by AWJ was investigated by Aydin et al. (2011). Engin (2012) investigated the effects of rock properties and operating parameters on the cutting depth of different natural stones machined by injection-type AWJ. The cutting depth was modeled using multiple linear and nonlinear regression analyses. Kim et al.

Arab J Geosci (2014) 7:4425–4435

(2012) analyzed the effect of traverse and rotational speed of the nozzle on the volume removal rate for concrete, granite, and obsidian samples machined by a suspension AWJ system. Engin et al. (2012) compared the cutting performance of AWJ and circular sawing based on specific energy expended per unit of volume of material removed during cutting. Using the Taguchi approach, the effects of process parameters on the cut depth of granite in AWJ cutting were investigated (Karakurt et al. 2012a). Statistically significant process parameters affecting the cut depth were determined. Aydin et al. (2012a) experimentally investigated the influence of textural properties (e.g., grain size and boundaries) of granite on the cutting performance of AWJ. Using regression analysis, models were developed by Aydin et al. (2012b) for the prediction of cut depth from operating variables and rock properties in AWJ machining of granitic rocks. Karakurt et al. (2012b) investigated the effects of AWJ operating variables on the kerf angle. They determined the significant material properties affecting the kerf angle. Karakurt et al. (2013) carried out an investigation on the kerf width in AWJ cutting of granitic rocks.

After an intense review of relevant literature, it is seen that no study has been conducted on significant rock parameters affecting the recycling of abrasives in AWJ machining of rock. The largest component of the operating costs is the abrasives, constituting nearly 75 % of the total operating expenses. When abrasive disposal is included, this percentage can be higher. The cost of abrasives has restricted many opportunities and usage of AWJ technology. With proper cleaning and sorting, an important portion of sludge can be recycled and fed back to the cutting process. Recycling abrasives makes the process more economical, effective, and environmentally friendly (Babu and Chetty 2003). In this study, it is aimed at attempting to fill this gap in the relevant literature.

Materials and method

Granites with different percentages of minerals, different grain size distributions and substantial market potential were

selected from a stone processing plant. The granite samples were dimensioned according to the requirements of the study at a length of 30 cm and 10 cm×3 cm sections. The tested granite samples are commercially termed as Verde Butterfly (R1), Giallo Fiorito (R2), Porto Rosa (R3), Crema Lal (R4), Giresun Vizon (R5), Balaban Green (R6), Bergama Gri (R7), Nero Zimbabwe (R8), and Star Galaxy (R9).

Physical properties of the tested granite samples are presented in Table 1. The specific mass (grams per cubic centimeter), water absorption by volume (percent), porosity (percent), ultrasonic velocity (meters per second), Schmidt hammer hardness, and Shore hardness are determined according to methods suggested by the International Society for Rock Mechanics (ISRM 1981). The microhardnesses of samples are measured by a Vickers Microhardness meter. A load of 100 g is chosen as recommended by Xie and Tamaki (2007). An average of three to five points is quoted as a value of microhardness of a mineral forming the rock. Then, the microhardness value of the mineral is multiplied with the proportion of the mineral forming the rock. The same procedure is followed for other minerals. Finally, the microhardness of each rock is determined as a total of these calculations. A similar procedure is applied for the determination of the Mohs' hardness of each rock sample. For Cerchar abrasiveness index (CAI) testing, a pointed steel pin having 610±5 Vickers hardness, 200 kg/mm^2 tensile strength, and a cone angle of 90° is applied to the surface of the rock samples for approximately one second under a static load of 68.646 N to scratch a 10 mm long groove. This procedure is repeated five times in various directions using a fresh pin for each repetition. The abrasiveness of the rock is determined by the resultant wear flat generated at the point of the stylus, which is measured in 0.1 mm units under a microscope. The unit of abrasiveness is defined as a wear flat of 0.1 mm which is equal to 1 CAI, ranging from 0 to 6 (Valantin 1974; Yarali and Kahraman 2011).

Thin sections of the samples were examined under a petrographic microscope for determining the mineral type and content. Polished hand specimens are also examined for grain size characterization of the coarse-grained rock samples.

Table 1 Physical properties of the rocks cut by AWJ

Rock properties	R1	R2	R3	R4	R5	R6	R7	R8	R9
Specific mass (g/cm^3)	2.81	2.71	2.69	2.64	2.72	2.72	2.66	3.09	2.90
Water absorption by volume (%)	0.20	0.28	0.30	0.86	0.20	0.19	0.30	0.14	0.10
Porosity (%)	1.50	0.80	1.50	1.50	3.30	2.20	1.80	0.30	1.00
Ultrasonic velocity (m/s)	4130	3917	4196	4140	5866	4849	4836	6054	6863
Cerchar abrasion index	4.348	4.166	4.508	5.2	3.868	4.356	4.622	3.412	4.29
Schmidt hammer hardness	47	48	51	56	54	55	54	64	65
Microhardness (HV)	502.04	543.47	538.73	539.55	505.5	559.03	537.93	501.84	463.18
Shore hardness	72.65	73.55	81.85	75.6	83.1	75.15	71.35	71.9	60.8
Mohs' hardness	6.1	5.7	6.0	4.5	6.0	6.0	6.3	6.2	5.8

Table 2 Mineralogical properties of the rocks

Rock type	Mineral	Grain size (mm)			Prop. (%)	Summary of petrographic description (texture, grain size)
		Min	Max	Mean		
R1	Alkali feldspar (orthoclase)	0.56	20.00	5.2	41	Allotriomorphic, very coarse-grained, grains between 0.08 and 20.0 mm
	Plagioclase	0.40	3.76	1.6	29	
	Quartz	0.16	6.00	2.5	11	
	Pyroxene	0.24	2.00	0.4	9	
	Biotite	0.32	3.60	1.5	6	
	Garnet	0.80	6.56	2.4	2	
	Opaque	0.08	0.80		2	
R2	Alkali feldspar (orthoclase, microcline)	0.80	18.00	12	41	Hypidiomorphic, very coarse-grained, grains between 0.08 and 18.0 mm
	Quartz	0.40	9.60	4	32	
	Plagioclase	0.40	2.40	1.8	14	
	Biotite	0.16	1.60	0.7	12	
	Secondary components	0.08	0.16		1	
R3	Alkali feldspar (orthoclase, microcline)	0.80	12.0	8	44	Allotriomorphic, very coarse-grained, grains between 0.16 and 12.0 mm
	Quartz	0.40	4.00	0.7	24	
	Plagioclase	0.96	6.80	1.7	24	
	Biotite	0.16	2.00	0.7	6	
	Other and secondary components (amphibole, apatite, zircon, opaque)	0.24	0.48		2	
R4	Alkali feldspar (orthoclase, microcline)	0.48	4.80	0.8	39	Hypidiomorphic, coarse-grained, grains between 0.08 and 4.80 mm
	Quartz	0.24	2.24	1.7	27	
	Plagioclase	0.56	3.60	2.0	22	
	Biotite	0.32	1.60	0.4	10	
	Secondary components	0.08	0.56		2	
R5	Alkali feldspar (orthoclase)	0.80	6.80	1.1	47	Allotriomorphic, coarse-grained, grains between 0.16 and 6.80 mm
	Plagioclase	0.32	4.88	2.2	27	
	Quartz	0.24	2.40	1.9	16	
	Amphibole	0.16	0.96	0.2	4	
	Biotite	0.48	3.44	1.4	4	
	Other and secondary components (pyroxene, apatite, zircon, opaque)	0.16	0.36		2	
R6	Alkali feldspar (orthoclase, microcline)	0.80	6.80	2.1	38	Hypidiomorphic, coarse-grained, grains between 0.08 and 6.80 mm
	Quartz	0.16	5.60	2.7	25	
	Plagioclase	0.96	5.20	2.2	14	
	Amphibole	0.24	1.20	0.4	10	
	Epidot	0.08	0.40	0.1	6	
	Biotite	0.48	3.20	0.7	4	
	Other and secondary components (mica, titanite, zircon, opaque)	0.16	0.96		3	
R7	Plagioclase	0.32	4.6	1.2	43	Hypidiomorphic, fine-grained, grains between 0.24 and 3.85 mm
	Alkali feldspar (orthoclase)	0.32	2.98	1.3	20	
	Quartz	0.24	3.60	1.2	19	
	Biotite	0.24	1.60	0.4	10	
	Amphibole	0.24	1.60	0.4	6	
	Other and secondary components (titanite, apatite, opaque)	0.24	0.80		2	
R8	Plagioclase	0.24	3.36	1.7	48	Hypidiomorphic, fine-grained, grains between 0.04 and 3.36 mm
	Pyroxene	0.24	2.40	1.6	40	
	Biotite	0.16	0.32	0.2	4	
	Opaque	0.04	0.80	0.1	8	
R9	Plagioclase	0.24	5.20	1.5	40	Hypidiomorphic, fine-grained, grains between 0.08 and 5.20 mm
	Pyroxene	0.24	3.60	1.3	39	
	Biotite	0.16	3.20	0.4	10	
	Amphibole	0.08	0.36	0.1	7	
	Other and sec. comp. (quartz and opaque)	0.08	1.36		4	

Fig. 1 A schematic illustration of the experimental setup (adopted from Duflou et al. [2001])
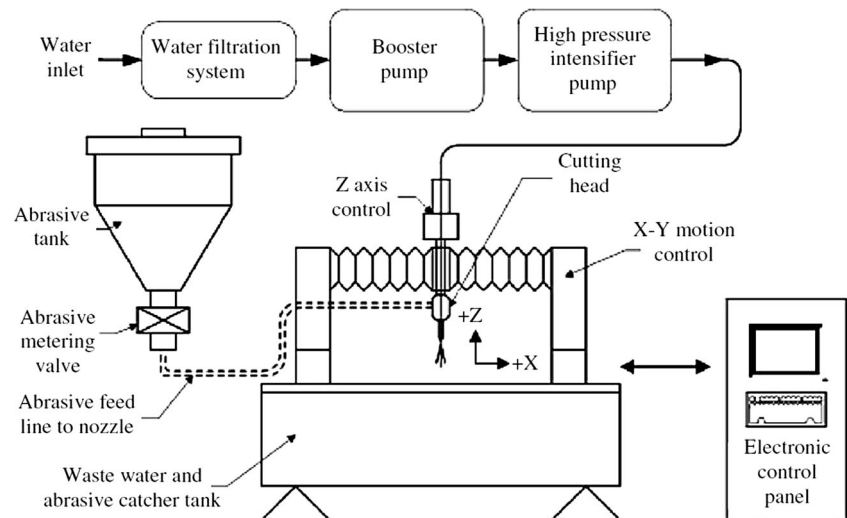
Moreover, the point-count method was employed for the modal analyses. These examinations mainly included the determination of modal compositions and grain size distributions of the rock samples. The mineralogical compositions of the rocks are given in Table 2 along with their textural and granular description. As can be followed from the table, quartz, alkali feldspar, plagioclase, and biotite were the main rock-forming minerals in all samples, varying in their percentage contents. Additionally, grain sizes of the rock-forming minerals were also determined using a digital image processing software of Dewinter Material Plus 4.1, and the mean grain size of the rock was then calculated.

A KMT International waterjet cutter equipped with a Model SL-V 50 HP intensifier pumping system is used for the cutting experiments, as schematically shown in Fig. 1. The motion of the nozzle is controlled by a computer as shown in the related figure. The nozzle diameter and length are 1.1 and 75 mm, respectively. The abrasives are delivered using compressed air from a hopper to the mixing chamber and are regulated using a metering disc. The debris of material and the slurry were collected into a catcher tank. Garnet chemically consisting of 36 % FeO, 33 % SiO_2, 20 % Al_2O_3, 4 % MgO, 3 % TiO_2, 2 % CaO, and 2 % MnO_2 is used as an abrasive material. Owing to the variability and accuracy of the

experimental data, each granite sample is cut five times through their lengths. In the study, the operating variables such as traverse speed, abrasive flow rate, standoff distance, and water pressure are kept constant (Table 3). These levels are selected based on previous works reported in literature on rock/rocklike cutting by an AWJ. After the cutting of each rock sample, the abrasive particles are gravitated while many of rock particles with excessive fragmentation are discharged from the tank with water. The gravitated abrasives and the remaining rock particles are then collected in a special container for following procedures. Gravity separation technique is employed to separate the abrasives and the rock particles having relatively lower gravities. To study the disintegration behavior of abrasives, abrasive particles are then dried and sieved. The abrasive particles are then dried for future procedures. The standard of 300, 212, 150, 106, 75, 53, 45, and 38 μm sieves are used to determine the particle size distribution. After classification, each series of abrasive particles are weighted. Petrographic microscope and scanning electron microscope (SEM, Zeiss Evo LS10) is used to study the changes in particle size and shape of abrasives after cutting of rock samples during various stages of recycling.

SPSS statistical software offers a choice of regression and is used in the study. Regression analysis includes many techniques for modeling and analyzing several variables, when the focus is on the relationship between a dependent variable and one or more independent variables. Specifically, regression analysis helps one understand how the typical value of the dependent variable changes when any one of the independent variables is varied, while other independent variables are held constant. Many techniques for carrying out regression analysis have been developed. Familiar methods such as linear regression and ordinary least squares regression are parametric. The regression function is defined in terms of a finite number of unknown parameters that are estimated from the data.

Table 3 Levels of the operating variables

Operating variables	Level
Traverse speed	100 mm/min
Abrasive flow rate	200 g/min
Standoff distance	4 mm
Water pressure	250 MPa
The commercial grade abrasive of mesh size	80 mesh
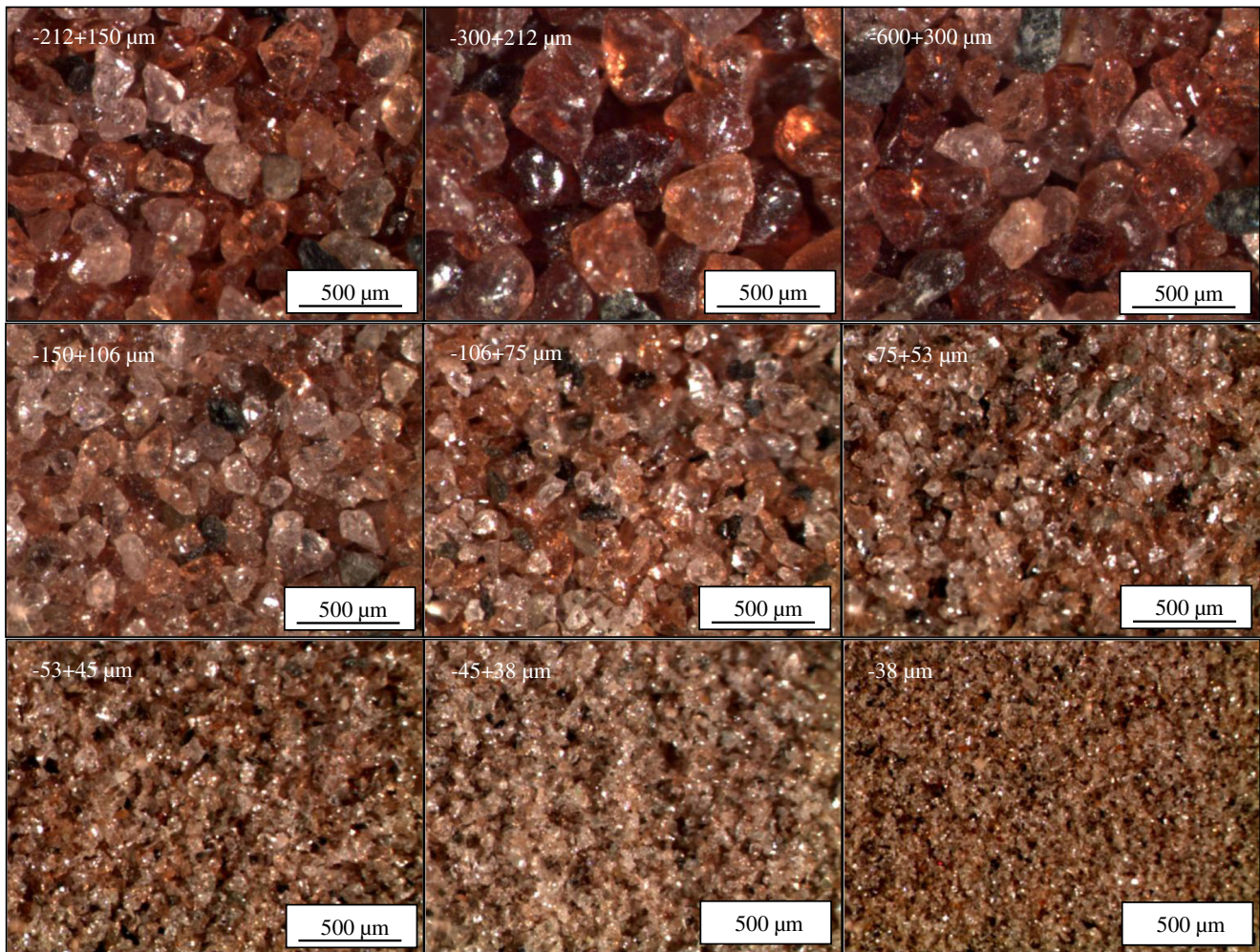
Fig. 2 The microscope images of the used abrasives in different size

Nonparametric regression refers to techniques that allow the regression function to lie in a specified set of functions, which may be infinite-dimensional (Armstrong 2012; Freedman 2005; Cook and Weisberg 1982). In this study, multiple regression analysis was employed. A multiple linear regression model is a hypothetical relationship and is described below.

Relevant independent variables defining the $AMP_{106\mu m}$ were selected to develop models that were obtained by means of regression models, which were validated and discussed for future predictions and reproducibility. Regression coefficients were estimated using the least-squares method. This method estimates the regression coefficients by minimizing the sum of

Table 4 The SEM/EDS observations for fresh abrasives

El	AN	Series	Unn. [wt.%]	C norm. [wt.%]	C atom. [at.%]	C error [%]
O	8	K-series	16.51	29.18	47.62	11.5
Mg	12	K-series	2.78	4.92	5.28	0.2
Al	13	K-series	7.03	12.43	12.03	0.4
Si	14	K-series	12.11	21.4	19.9	0.5
Ca	20	K-series	0.47	0.83	0.54	0
Ti	22	K-series	0.17	0.31	0.17	0
Mn	25	K-series	0.55	0.97	0.46	0.1
Fe	26	K-series	16.94	29.95	14	0.5
Total:			56.56	100	100	

Table 5 The SEM/EDS observations for used abrasives

El	AN	Series	Unn. [wt.%]	C norm. [wt.%]	C atom. [at.%]	C error [%]
O	8	K-series	30.49	45.53	65.2	25.6
Mg	12	K-series	2	2.99	2.82	0.1
Al	13	K-series	5.99	8.95	7.6	0.3
Si	14	K-series	10.14	15.15	12.36	0.5
Ca	20	K-series	3.09	4.62	2.64	0.1
Ti	22	K-series	0.41	0.61	0.29	0.1
Mn	25	K-series	0.72	1.07	0.45	0.1
Fe	26	K-series	14.12	21.08	8.65	0.5
Total			66.96	100	100	

the squares of the deviations to the proposed regression model (Aranda et al. 2012).

A regression equation is as shown:

$$\widehat{Y} = \beta_0 + \beta_1 x_1 + \beta_2 x_2 + \ldots + \beta_p x_p \quad (1)$$

Where $\widehat{Y}$ is the fitted value and β_0, β_1… and β_p are the estimations of the regression parameters.

The real value for Y is:

$$Y = \beta_0 + \beta_1 x_1 + \beta_2 x_2 + \ldots + \beta_p x_p + \varepsilon \quad (2)$$

Where ε is the random error.

β_0, β_1…, and β_p describe the expected change in the predicted variable Y in response to a unitary change in x_i when the rest of predictors remain constant.

Results and discussion

An optical examination was performed, and the pictures for each particle size are presented in Fig. 2. The SEM and energy dispersive X-ray analysis (EDS) observations for fresh and used abrasives are also summarized in Tables 4 and 5, followed by SEM micrographs and EDS spectra, shown in Figs. 3
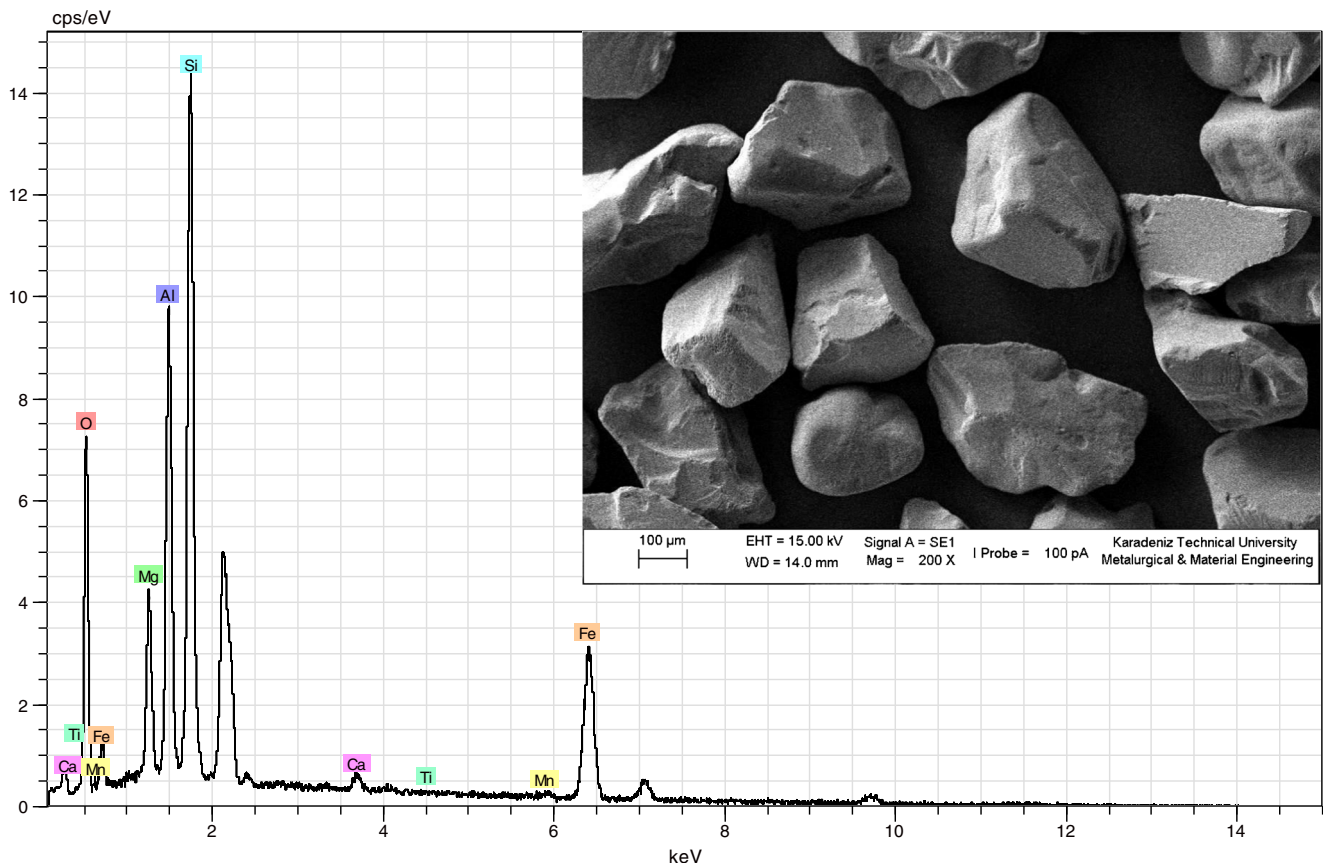
Fig. 3 SEM micrographs and EDS spectra for the fresh abrasives

and 4, respectively. The figures indicate that the abrasive is predominantly composed of Fe and Si.

Particle size distribution of the used abrasives and the $AMP_{106\mu m}$ for each kind of rock are depicted in Fig. 5. This figure exhibits a considerable amount of abrasives that are present above 106 μm (66.71–92.20 %), which can be effectively used again in the rock cutting applications. However, some deformations (Fig. 4) formed during the cutting was observed in range of −106 μm having an amount such as 7.80–33.29 %. The highest size reduction in the abrasives was observed for Star Galaxy, which is followed by Verde Butterfly, Nero Zimbabwe, Giresun Vizon, Bergama Gri, Crema Lal, Porto Rosa, Giallo Fiorito, and Balaban Green.

In the following analysis, the $AMP_{106\mu m}$ is considered as a performance criterion in terms of recycling of abrasives. Regression analysis is carried out to determine relationships among the $AMP_{106\mu m}$ and the physical properties of rock such as specific mass, water absorption by volume, porosity, Schmidt hammer hardness, ultrasonic velocity, Cerchar abrasion index, microhardness, Shore hardness, and Mohs' hardness. Table 6 presents the regression equations with determination coefficients. Among the physical properties, a powerful correlation between the $AMP_{106\mu m}$ and the microhardness

was found. Therefore, it is noted that microhardness can be a useful property for estimating the $AMP_{106\mu m}$ affecting the recycling of abrasives in AWJ cutting for different types of granites. Relationships between the $AMP_{106\mu m}$ and some mineralogical properties of rock such as mineralogical content, mean and maximum grain size of minerals, and mean grain size of rock are also investigated (Table 7). Table 7 indicates that reliable correlations were found between the $AMP_{106\mu m}$ and the quartz content. Higher $AMP_{106\mu m}$ values were generally obtained for the rocks including lower percentage of quartz. A moderate correlation was also found between the $AMP_{106\mu m}$ and the plagioclase content.

Development of models for $AMP_{106\mu m}$ prediction

As a result of multiple regression analysis, it was determined that the $AMP_{106\mu m}$ can be predicted from eight independent variables, which includes uniaxial strength (megapascals), Shore hardness, microhardness (HV), Mohs' hardness, maximum grain size of plagioclase (millimeters), mean grain size of plagioclase (millimeters), mean grain size of alkali feldspar (millimeters), and mean grain size of biotite (millimeters). The
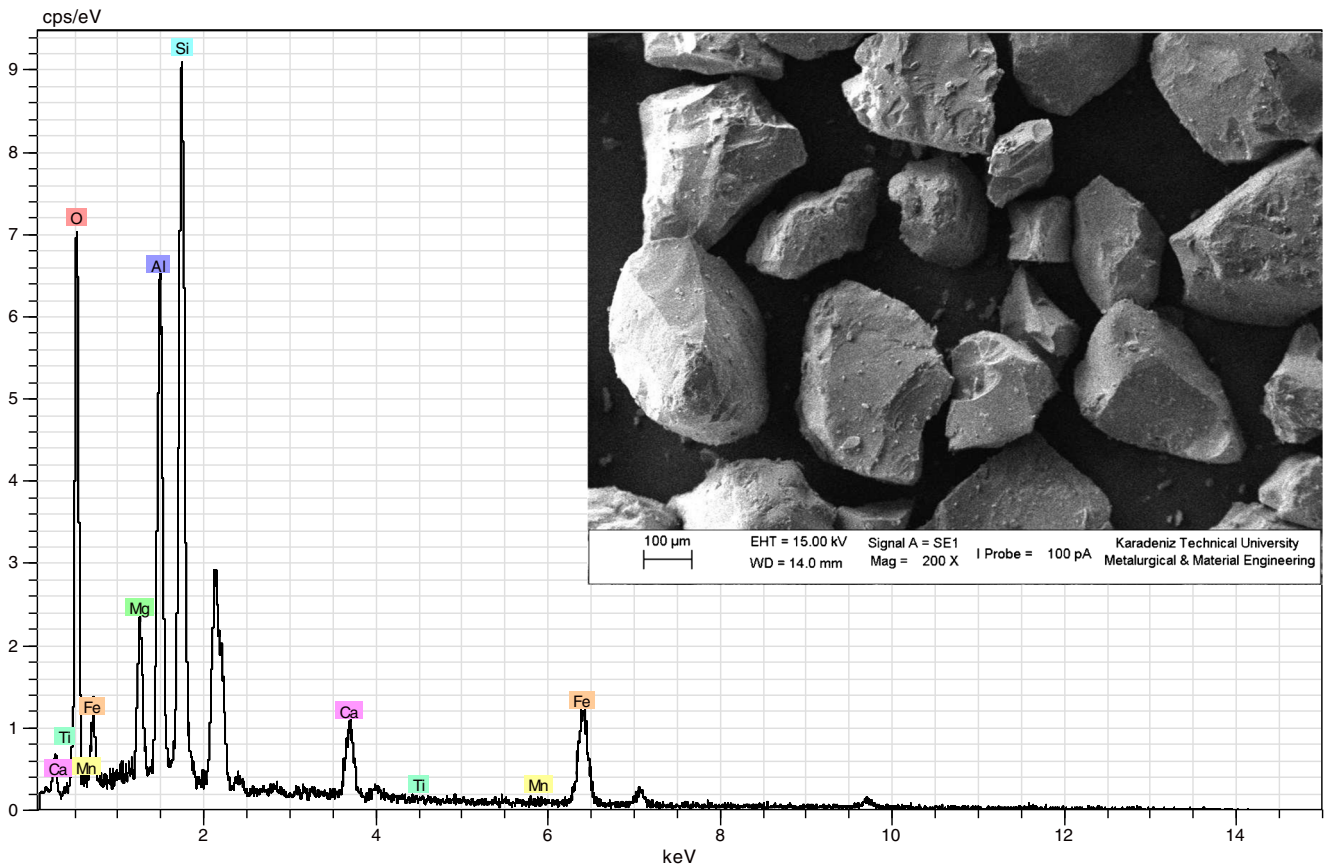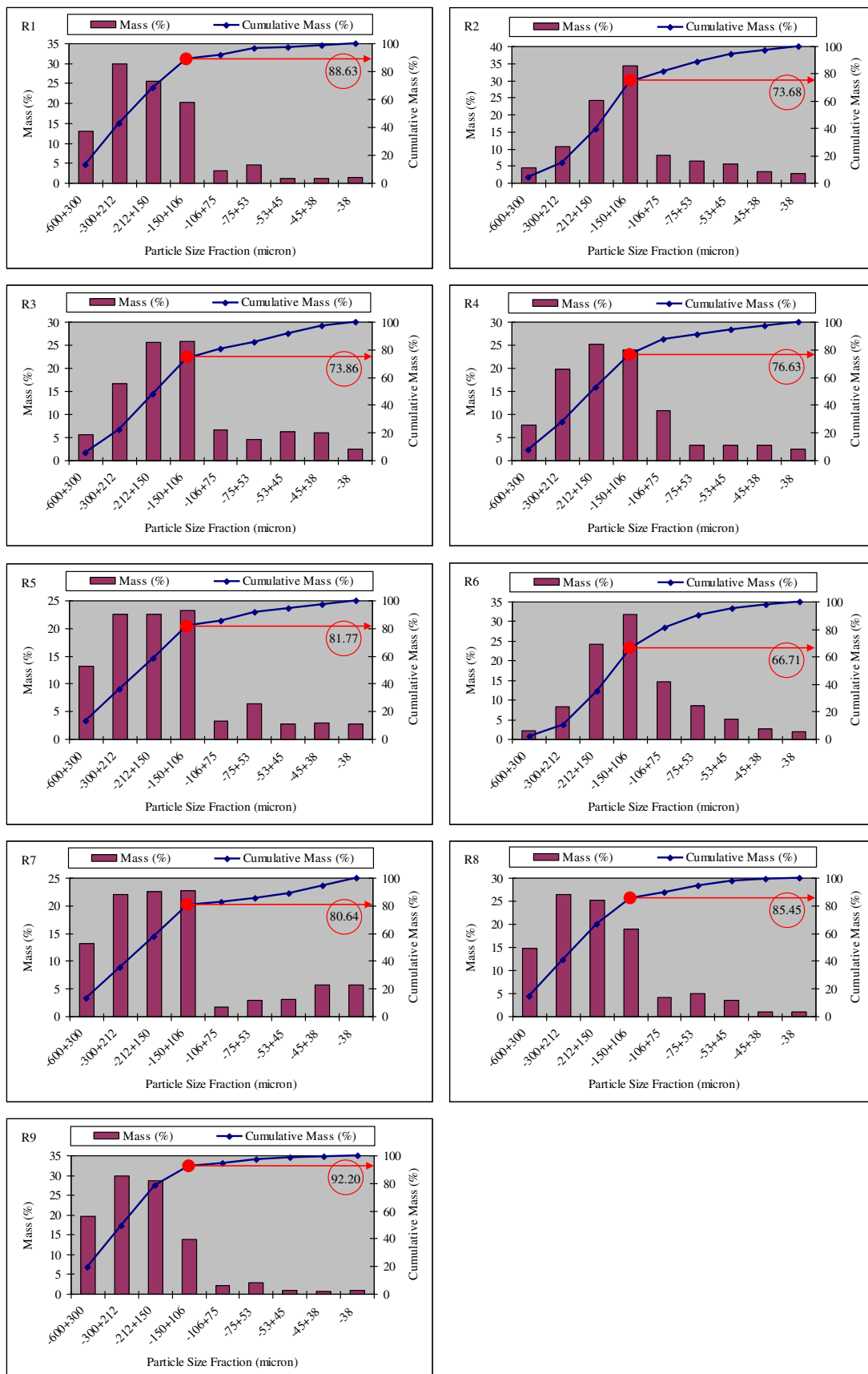

Fig. 4 SEM micrographs and EDS spectra for the used abrasives

Fig. 5 The particle size distribution of the used abrasives and determination of $AMP_{106\mu m}$

Table 6 Relationships between $AMP_{106\mu m}$ and physical properties

Rock properties	Regression equation	Determination coefficient R^2
Specific weight (g/cm³)	$y=33.29x-12.31$	0.349
Water absorption by volume (%)	$y=-11.362x+83.196$	0.101
Porosity (%)	$y=-2.3618x+83.599$	0.064
Schmidt hammer hardness	$y=0.5274x+51.006$	0.167
Ultrasonic velocity (m/s)	$y=0.0045x+57.554$	0.336
Shore hardness	$y=-0.7018x+131.88$	0.317
Cerchar abrasion index	$y=-4.7618x+100.46$	0.085
Microhardness (HV)	$y=-0.2511x+210.83$	0.870
Mohs' hardness	$y=3.1117x+61.75$	0.043

determination coefficient of Eq. 3 is 1. Thus, means 100 % of the variation of the experimental data is explained by the equation. The related regression analysis is:

$$AMP_{106mm} = 0.019 X_1 + 0.184 X_2 - 0.196 X_3 - 0.887 X_4$$
$$-0.824 X_5 - 12.153 X_6 - 0.364 X_7 + 3.883 X_8 \quad (3)$$

Where;

X_1: Uniaxial strength (megapascals), X_2: Shore hardness, X_3: Microhardness (HV), X_4: Mohs' hardness, X_5: Maximum grain size of plagioclase (millimeters), X_6: Mean grain size of plagioclase (millimeters), X_7: Mean grain size of alkali feldspar (millimeters), X_8: Mean grain size of biotite (millimeters).

Although Eq. 3 has the highest correlation coefficients, it may not be useful due to its complexity and impracticality. Therefore, the $AMP_{106\mu m}$ was modeled as a function of some rock properties having relatively higher correlations with $AMP_{106\mu m}$. The developed model and the results of the statistical analysis are presented in Table 8. The analysis suggests

that the $AMP_{106\mu m}$ is explained by microhardness, quartz content, and plagioclase content with high accuracy (Eq. 4).

$$AMP_{106mm} = 206.684 - 0.268 X_1 + 0.285 X_2 + 0.268 X_3 \quad (4)$$

Where;

X_1: Microhardness (HV), X_2; Plagioclase content (percent), and X_3: Quartz content (percent).

Model validation is necessary and provides a good indication on the accuracy and generality of the models developed. Therefore, several validation methods including model determination coefficient (R^2), plots of observed and predicted $AMP_{106\mu m}$, t test, F test, and residual analysis are used for verification of the models.

The R^2 value for the model is 0.927, indicating a high degree of relationship between the $AMP_{106\mu m}$ and the study variables. The coefficient of determination also indicates that 0.073 % of the variation in the $AMP_{106\mu m}$ is due to all causes other than the predictors as they appear in Eq. 2. Equivalently, 0.073 % variation in the $AMP_{106\mu m}$ remains unexplained. The generality and reliability of the models are further studied by examining predicted trends versus observed trends as shown in Fig. 6. The predicted $AMP_{106\mu m}$ values are very close to the actual ones.

In the analysis, the F test is used to examine the significance of each model and a t test is used for each variable at a 95 % significance level. The models that have a larger F-ratio than the F-ratio from the statistical tables are considered statistically significant. The models that have a smaller F-ratio than the F-ratio from the statistical tables are considered statistically insignificant. Similarly, if the variable in a model has a larger t value than the t value from the statistical table, the variable is considered statistically significant. If the variable has smaller t value than the t-value from the statistical table, the variable is considered statistically insignificant. The

Table 7 Relationships between $AMP_{106\mu m}$ and mineralogical properties

Rock properties	Regression equation	Determination coefficient R^2
Plagioclase content (%)	$y=0.4907x+65.721$	0.556
Alkali feldspar content (%)	$y=-0.2537x+87.561$	0.341
Quartz content (%)	$y=-0.5963x+90.154$	0.719
Biotite content (%)	$y=0.159x+78.786$	0.004
Mean GS of plagioclase (mm)	$y=-12.793x+102.55$	0.269
Mean GS of alkali feldspar (mm)	$y=-0.7624x+82.535$	0.155
Mean GS of quartz (mm)	$y=-2.6584x+84.648$	0.153
Mean GS of biotite (mm)	$y=1.5656x+78.838$	0.008
Mean GS of rock (mm)	$y=-1.5668x+83.85$	0.130
Maximum GS of plagioclase (mm)	$y=-0.78x+83.4$	0.016
Maximum GS of alkali feldspar (mm)	$y=-0.2441x+81.887$	0.049
Maximum GS of quartz (mm)	$y=-1.362x+85.218$	0.236
Maximum GS of biotite (mm)	$y=0.9547x+77.77$	0.018

Table 8 Statistical results of the MLRA

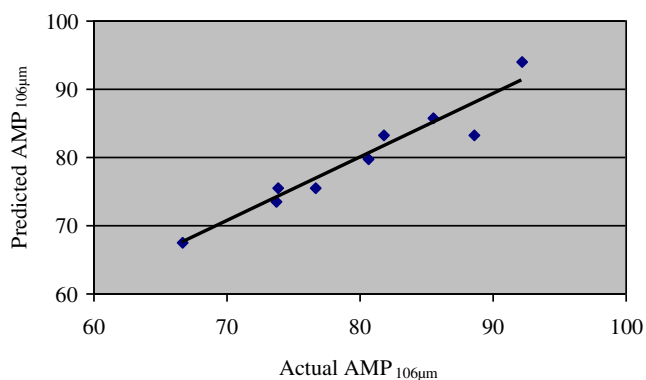| Coefficients	Unstandardized coefficients		Standardized coefficients	t	F	R square	Adjusted R square	Std. error of the estimate	Tabulated t value	Tabulated F-ratio
	B	Std. error								
Constant	206.684	33.327		6.202	21.012	0.927	0.882	2.771	1.729	3.13
Microhardness	−0.268	0.073	−0.995	−3.693						
Plagioclase cont.	0.285	0.150	0.433	2.920						
Quartz cont.	0.268	0.259	0.382	1.950						

computed F and t values for the models are greater than the tabulated F and t values, indicating that the proposed models are statistically valid (Table 8).

The direct comparison of model and real data in the form of residuals is another validation method that is used for checking models verification. This method provides indications about the appropriateness of a model. This technique provides more effective test for proving and detecting abnormal behavior in residuals. Therefore, scatter plots were studied to investigate the distribution of residuals. In general, the residuals depicted in Fig. 7 are randomly scattered around the line confirming the correctness of the model. Model results revealed that the proposed model has a high potential for the estimation of the $AMP_{106\mu m}$. For future applications, the $AMP_{106\mu m}$ can be effectively estimated by the proposed model.

Conclusions

In this experimental study, significant rock parameters affecting the recycling of abrasives in AWJ machining were determined. Some specific findings of the present study are given below:

1. According to the rock types, 66.71–92.20 % of the used abrasive was still present in useable form.
2. Among rock properties, a strong correlation was found between the $AMP_{106\mu m}$ and microhardness. A relatively lower correlation was found between quartz content and the $AMP_{106\mu m}$. This indicates that quartz content alone may not be a major contributor to the $AMP_{106\mu m}$. It is therefore reasonable to suggest that rather than the quartz content of the rock, microhardness could primarily be responsible for the $AMP_{106\mu m}$. Therefore, it can be noted that microhardness is a useful property for the $AMP_{106\mu m}$, which affects the recycling of abrasives in the cutting of the rocks by AWJ.
3. The $AMP_{106\mu m}$ can be explained by microhardness, quartz content, and plagioclase content with high accuracy. The determination coefficient of the proposed model is 0.927, indicating a strong relationship between the $AMP_{106\mu m}$ and the study variables. This model suggests that the combined effect of all individual mineralogical and physico-mechanical properties of granitic rocks should be evaluated before a final decision is made on the $AMP_{106\mu m}$.
4. The proposed models are statistically valid in terms of the t test and F test. Accuracy of the models is also confirmed by the residuals.

For future research, investigating the effect of operating variables on the $AMP_{106\mu m}$ and determining dominant operating variables affecting the $AMP_{106\mu m}$ can be conducted. The rock cutting performances of recovered abrasives also can be determined in terms of the cutting depth, width, angle, and the surface roughness of the rock cut.

Fig. 6 Actual $AMP_{106\mu m}$ versus predicted $AMP_{106\mu m}$
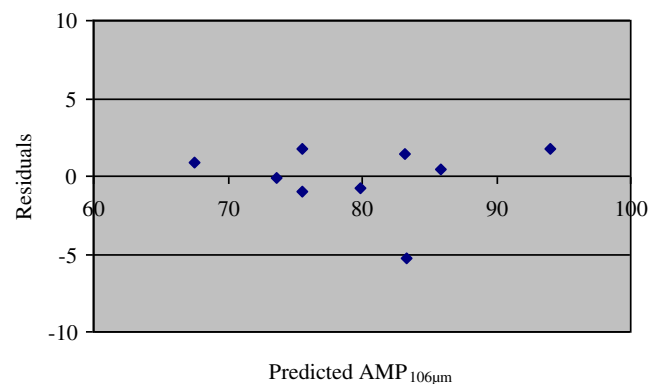
Fig. 7 Residuals against the predicted $AMP_{106\mu m}$

References

Aranda A, Ferreira G, Mainar-Toledo DM, Scarpellini S, Sastresa LE (2012) Multiple regression models to predict the annual energy consumption in the Spanish banking sector. Energ Build 49:380–387

Armstrong SJ (2012) Illusions in regression analysis. Int J Forecast 28(3): 689–694

Ataei M, Mikaiel R, Sereshki F, Ghaysari N (2012) Predicting the production rate of diamond wire saw using statistical analysis. Arab J Geosci 5(6):1289–1295

Aydin G, Karakurt I, Aydiner K (2011) An investigation on the surface roughness of the granite machined by abrasive waterjet. Bull Mater Sci 34(4):985–992

Aydin G, Karakurt I, Aydiner K (2012a) Cutting performance of abrasive waterjet in granite: Influence of the textural properties. J Mater Civil Eng 24(7):944–949

Aydin G, Karakurt I, Aydiner K (2012b) Prediction of cut depth of the granitic rocks machined by abrasive waterjet (AWJ). Rock Mech Rock Eng. doi:10.1007/s00603-012-0307-1

Babu KM, Chetty KOV (2003) A study on recycling of abrasives in abrasive water jet machining. Wear 254:763–773

Bayram F (2012) Prediction of sawing performance based on index properties of rocks. Arab J Geosci. doi:10.1007/s12517-012-0668-5

Brook N, Summers DA (1969) The penetration of rock by high-speed water jets. Int J Rock Mech Min 6(3):249–258

Chakravarthy SP, Babu RN (1999) A new approach for selection of optimal process parameters in abrasive water jet cutting. Mater Manuf Process 14(4):581–600

Chakravarthy PS, Babu AR, Babu NR, (1998) A fuzzy based approach for selection of process parameters in abrasive waterjet cutting of black granite. In: Proc. of 5th Pacific Rim international conference on water jet technology, New Delhi, India, pp 108–120

Ciccu R, Grosso B (2010) Improvement of the excavation performance of PCD drag tools by waterjet assistance. Rock Mech Rock Eng 43: 465–474

Cook D, Weisberg S (1982) Criticism and influence analysis in regression. Sociol Methodol 13:313–361

Duflou JR, Kruth JP, Bohez EL (2001) Contour cutting of pre-formed parts with abrasive waterjet using 3-axis nozzle control. J Mater Process Technol 115:38–43

Engin CI (2012) A correlation for predicting the abrasive water jet cutting depth for natural Stones. S Afr J Sci 108(9/10):1–11

Engin CI, Bayram F, Yasitli EN (2012) Experimental and statistical evaluation of cutting methods in relation to specific energy and rock properties. Rock Mech Rock Eng. doi:10.1007/s00603-012-0284-4

Freedman AD (2005) Statistical models: Theory and practice, Cambridge University Press

Hlavac LM, Hlavacova IM, Gembalova L et al (2009) Experimental method for the investigation of the abrasive water jet cutting quality. Int J Mater Process Technol 209(20):6190–6195

ISRM (1981) Rock characterization testing and monitoring suggested methods. In: Brown ET (Ed) Oxford, Pergamon Press, pp. 211

Karakurt I, Aydin G, Aydiner K (2012a) An experimental study on the cut depth of the granite in abrasive waterjet cutting. Mater Manuf Process 27(5):538–544

Karakurt I, Aydin G, Aydiner K (2012b) A study on the prediction of kerf angle in abrasive waterjet machining of rocks. Proc Inst Mech Eng B J Eng 226:1489–1499

Karakurt İ, Aydın G, Aydıner K (2013) An investigation on the kerf width in abrasive waterjet cutting of granitic rocks. Arab J Geosci. doi:10.1007/s12517-013-0984-4

Kim GJ, Song JJ, Han SS et al (2012) Slotting of concrete and rock using an abrasive suspension waterjet system. KSCE J Civ Eng 16(4): 571–578

Mikaeil R, Ataei M, Yousefi R (2013) Correlation of production rate of ornamental stone with rock brittleness indexes. Arab J Geosci 6: 115–121

Miranda MR, Quintino L (2005) Microstructural study of material removal mechanisms observed in abrasive waterjet cutting of calcareous Stones. Mater Charact 54(4–5):370–377

Nikonov GP, Goldin YA (1972) Coal and rock penetration by fine continuous high pressure water jets. In: Proc. 1st. International Symposium on Jet Cutting Technology

Pon Selvan CM, Raju SMN (2011) Assessment of process parameters in abrasive waterjet cutting of granite. International Conference on Trends in Mechanical and Industrial Engineering (ICTMIE'2011) Bangkok, pp. 140–144

Sengun N, Altindag R (2013) Prediction of specific energy of carbonate rock in industrial stones cutting process. Arab J Geosci 6(4):1183–1190

Valantin A (1974) Examen des différent procèdes classiques de la nocivité des roches vis-à-vis de l'abatage mécanique. Industrie Minérale Mine; 133–140

Xiaohong L, Jiansheng W, Yiyu L et al (2000) Experimental investigation of hard rock cutting with collimated abrasive water jets. Int J Rock Mech Min 37:1143–1148

Xie J, Tamaki J (2007) Parameterization of micro-hardness distribution in granite related to abrasive machining performance. J Mater Process Technol 186:253–258

Yarali O, Kahraman S (2011) The drillability assessment of rocks using the different brittleness values. Tunn Undergr Space Technol 26: 406–414